

Microcephalin coordinates mitosis in the syncytial *Drosophila* embryo

Kathrin Brunk^{1,2,3,*}, Bertrand Vernay^{3,*}, Elen Griffith³, Natalie L. Reynolds³, David Strutt², Philip W. Ingham² and Andrew P. Jackson^{3,‡}

¹Institute of Integrative and Comparative Biology, University of Leeds, LS2 9JT, UK

²MRC Centre for Developmental and Biomedical Genetics, University of Sheffield, S10 2TN, UK

³MRC Human Genetics Unit, Western General Hospital, Edinburgh, EH4 2XU, UK

*These authors contributed equally to this work

‡Author for correspondence (e-mail: andrew.jackson@hgu.mrc.ac.uk)

Accepted 24 July 2007

Journal of Cell Science 120, 3578-3588 Published by The Company of Biologists 2007

doi:10.1242/jcs.014290

Summary

Microcephalin (*MCPHI*) is mutated in primary microcephaly, an autosomal recessive human disorder of reduced brain size. It encodes a protein with three BRCT domains that has established roles in DNA damage signalling and the cell cycle, regulating chromosome condensation. Significant adaptive evolutionary changes in primate *MCPHI* sequence suggest that changes in this gene could have contributed to the evolution of the human brain. To understand the developmental role of microcephalin we have studied its function in *Drosophila*. We report here that *Drosophila* *MCPHI* is cyclically localised during the cell cycle, co-localising with DNA during interphase, but not with mitotic chromosomes. *mcp1* mutant flies have a maternal effect lethal phenotype, due to mitotic arrest occurring in early syncytial cell cycles. Mitotic entry is slowed from the very first mitosis in such embryos, with

prolonged prophase and metaphase stages; and frequent premature separation as well as detachment of centrosomes. As a consequence, centrosome and nuclear cycles become uncoordinated, resulting in arrested embryonic development. Phenotypic similarities with *abnormal spindle* (*asp*) and *centrosomin* (*cnn*) mutants (whose human orthologues are also mutated in primary microcephaly), suggest that further studies in the *Drosophila* embryo may establish a common developmental and cellular pathway underlying the human primary microcephaly phenotype.

Supplementary material available online at
<http://jcs.biologists.org/cgi/content/full/120/20/3578/DC1>

Key words: *Drosophila* embryo, Microcephalin, Centrosome, Mitosis

Introduction

Mutation in microcephalin (*MCPHI*) causes primary microcephaly (MIM#251200), an autosomal recessive disorder of human brain size in which brain volume is reduced to a third of normal, a size comparable with that of early hominids (McCreary et al., 1996; Wood and Collard, 1999; Woods et al., 2005). Comparative genomic sequencing has established that significant adaptive evolutionary changes have occurred in microcephalin in primates, in the lineage from the last common simian ancestor to man (Evans et al., 2004; Wang and Su, 2004). It has thus been suggested that changes in this gene could have contributed to the evolution of the human brain.

Microcephalin (*MCPHI*) is the first of four disease genes to be identified for this condition (Jackson et al., 2002) and encodes an 835 amino acid protein containing 3 BRCA1 C-terminal (BRCT) domains (Huyton et al., 2000). Such domains can bind other proteins in a phosphorylation-dependent manner (Yu et al., 2003), explaining their presence in many proteins involved in DNA repair and regulation of cell cycle (Huyton et al., 2000), processes dependent on phosphorylation signals. Subsequently microcephalin has been found to have multiple roles in cell cycle and DNA repair. Microcephalin has been implicated in the timing of cell cycle events and specifically in the regulation of chromosome condensation (Neitzel et al., 2002; Trimborn et al., 2004) and Cdk1 phosphorylation (Alderton et al., 2006). Both RNAi depletion and mutation of

microcephalin result in a cellular phenotype of premature chromosome condensation (Neitzel et al., 2002; Trimborn et al., 2004). This is the consequence of premature onset of chromosome condensation, mediated by condensin II in G2 and delayed decondensation after mitosis (Trimborn et al., 2004; Trimborn et al., 2006), and correlates with the loss of inhibitory Cdk1 phosphorylation in S and G2 in microcephalin-deficient cells (Alderton et al., 2006). In the context of DNA repair, microcephalin has been found to be a chromatin-associated protein that also colocalizes with DNA repair proteins at ionizing radiation-induced DNA repair foci (Lin et al., 2005; Rai et al., 2006; Xu et al., 2004). It is required for intra-S and G2-M checkpoints (Lin et al., 2005; Xu et al., 2004), and acts downstream of Chk1 in the ATR signalling cascade regulating Cdc25A stability, and consequently G2-M transition (Alderton et al., 2006).

Three other primary microcephaly genes have been identified, *ASPM*, *CENPJ* and *CDK5RAP2* (Bond et al., 2002; Bond et al., 2005). All their proteins have a centrosomal localization, and *Drosophila* orthologues that are required for centrosomal function: *Abnormal spindle* (*Asp*), *Sas-4* and *Centrosomin* (*Cnn*), respectively (Basto et al., 2006; Gonzalez et al., 1990; Megraw et al., 1999; Riparbelli et al., 2002; Vaizel-Ohayon and Schejter, 1999). *Asp* is required for the integrity of centrosomes as microtubule-organizing centres, focusing the spindle poles at mitosis (do Carmo Avides and Glover, 1999).

Cnn is essential for the localisation of other centrosomal components, gamma tubulin, CP190 and CP60 (Megraw et al., 1999; Vaizel-Ohayon and Schejter, 1999), whereas Sas-4 is necessary for centriole duplication, with mutant flies consequently lacking centrosomes, cilia and flagella (Basto et al., 2006). Despite these important cellular functions, all three mutants can generate morphologically normal adults, though *sas-4* mutants die shortly after birth as they lack sensory neurons. *asp* and *cnn* have maternal-effect lethal alleles in which mitotic arrest occurs in embryonic cell cycles prior to cellularisation (Gonzalez et al., 1990; Megraw et al., 1999). Defects in localisation of asymmetric determinants have also been observed in *cnn* and *sas-4* neuroblasts (Basto et al., 2006; Megraw et al., 2001).

Overall, there is a unifying theme for primary microcephaly of genes functioning in processes of cell division. It has therefore been proposed that reduced brain size is the result of reduced 'neurogenic' mitosis, perhaps as a consequence of perturbed neural progenitor asymmetric cell division (Cox et al., 2006). However, microcephalin's function has appeared to be distinct from the other genes, and so we have generated a *Drosophila* model for microcephalin, to characterise its developmental role and to examine its mitotic functions. We report here the identification of *Drosophila microcephalin* (*mcpH1*), establish that *mcpH1* mutants have a maternal effect lethal phenotype and determine that a short isoform of microcephalin is required for the co-ordination of syncytial centrosomal and nuclear division cycles.

Results

Drosophila mcpH1 is the orthologue of human microcephalin

The *Drosophila melanogaster* homologue of microcephalin was identified by TBLASTN (Altschul et al., 1990) searches of the *Drosophila* genomic and EST databases using the human protein sequence (CAC34661). We predicted a transcript, *mcpH1(L)*, corresponding to the human microcephalin protein that combines two adjacent annotated genes (*CG8981* and *CG30038*) on chromosome 2R at 48C5 (Fig. 1). This transcript was confirmed by RT-PCR and sequencing of adult testis mRNA (Fig. S1, supplementary material). The nine exon *mcpH1* gene encodes a 1028 amino acid protein sharing 18% amino acid identity with human microcephalin (Fig. S2 supplementary material). Like its human counterpart, *Drosophila* MCPH1 has a unique pattern of BRCT domains, with a single N-terminal and tandem C-terminal BRCT domains, and is predicted to be a nuclear protein (PSORT II) (Nakai and Horton, 1999).

mcpH1 splice variants

mcpH1 has two sites of alternative splicing at intron 1 and 7, potentially resulting in four processed transcripts (Fig. 1A). The fully spliced transcript encodes the longest protein isoform, MCPH1(L), that contains all three BRCT domains (Fig. 1B,C). This transcript was experimentally validated as described above (Fig. S1 supplementary material). A second transcript, *mcpH1(S)*, encodes a short (S) variant of MCPH1 containing only one functional, N-terminal BRCT domain (Fig. 1B,C). This transcript contains an unspliced intron 7, resulting in a premature stop codon, and corresponds to the annotated CG8981-RB gene (FlyBase). We confirmed this

transcript through re-sequencing of a full-length cDNA clone from the *Drosophila* Genomic Collection (LD43341, AY122187).

EST data also suggests the presence of other *mcpH1* transcripts with an unspliced intron 1 and an alternative translational start site (Fig. 1A) that results in a different, shorter N-terminal coding sequence. In combination with alternative splicing of intron 7, these would encode two further proteins. These proteins would have domain structures similar to MCPH1(S) and MCPH1(L), but be shorter by 47 amino acids at their N termini (one of these proteins is annotated on FlyBase as CG8981-RA). We experimentally confirmed the existence of unspliced intron 1 transcripts, which appear to be present in all developmental stages (data not shown). Unlike the intron 7 alternative splicing, the intron 1 splicing is not predicted to alter domain structure; we therefore focused our subsequent analysis on the 'full length' MCPH1(L) and MCPH1(S) proteins.

mcpH1(S) is expressed during early cleavage stages

RT-PCR experiments established that *mcpH1* transcripts are present at all developmental stages from embryo to adults (data not shown). Whole-mount in situ hybridisation of wild-type embryos was performed using a riboprobe common to both L and S transcripts. This detected *mcpH1* mRNA at its highest level in syncytial stages, distributed throughout the embryo. By the cellular blastoderm stage minimal *mcpH1* transcript was apparent, consistent with *mcpH1* being maternally derived until cellularisation and midblastula transition (Fig. 1D). During gastrulation, *mcpH1* transcript is again detectable, presumably as a result of zygotic expression of the gene.

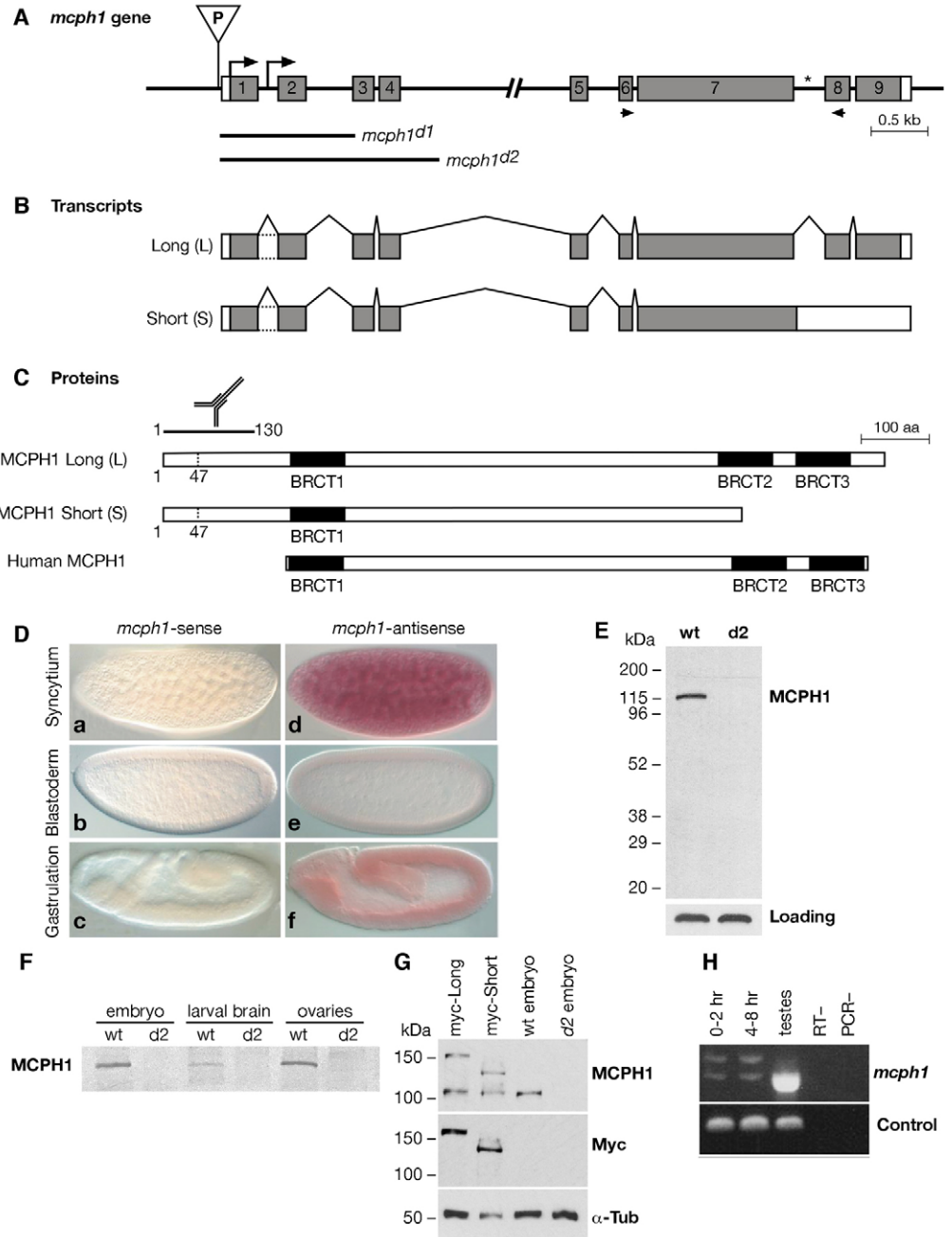
To characterise MCPH1 protein expression, polyclonal rabbit antibodies were raised against an N-terminal fragment of the protein (Fig. 1C, antibody symbol). The affinity purified antibody detected a single specific 115 kDa band in immunoblots performed on extracts of syncytial embryos that is not present in embryos derived from mothers homozygous for a *mcpH1* deletion (*mcpH1^{d2/d2}*), hereafter referred to as *mcpH1^{d2/d2}* embryos (Fig. 1E). This protein was also present in ovaries and at reduced levels in larval brain (Fig. 1F, and data not shown). This band corresponds to the predicted molecular mass of the L isoform; however, human microcephalin protein migrates significantly slower than predicted, so the 115 kDa band could represent a shorter isoform.

To determine which isoform is present in syncytial embryos, we cloned the MCPH1 S and L isoforms of the gene into pPMW (from Terence Murphy), an epitope-tagged (6xMyc) pUASP vector, using the Gateway system (Invitrogen). These transgenes were then expressed in embryos using the *mat α Tub67::Gal4VP16* maternal driver and the protein mobility compared with endogenous protein (Fig. 1G). Correcting for the additional molecular mass of the epitope tag, the transgenic MCPH1(S) protein exhibits similar mobility to the endogenous embryonic protein, whereas the MCPH1(L) transgenic protein is substantially larger than endogenous protein. We also examined *mcpH1* transcripts by RT-PCR, and established that both spliced and unspliced intron 7 transcripts are present in embryos, whereas in testis only the fully spliced isoform is detectable (Fig. 1H).

Taken together, these data indicate that MCPH1(S), the shorter isoform of microcephalin is present in the syncytial

Fig. 1. *Drosophila microcephalin*.

(A) Genomic organisation of *mcpH1*. Schematic drawing illustrating exons (boxed), coding sequence (grey shading) and P{GawB}NP6229 insertion site (triangle). Translational start sites (arrows) are present in exon 1, and intron 1 (for transcripts with unspliced intron 1). Variable splicing in intron 7 results in a second premature stop codon (asterisk). Deleted regions in the *mcpH1^{d1}* and *mcpH1^{d2}* mutants, generated by imprecise excision of the P{GawB}NP6229 element are marked by black bars. The *mcpH1^{d1}* deletion is 1210 bp from the P insertion site to coding base pair 626 in exon 3. *mcpH1^{d2}* deletion extends 1649 bp from the P insertion site to intron 4. (B) Schematic drawings showing the organisation of the *mcpH1* transcripts and (C) proteins. The long (L) isoform contains three BRCT domains (black boxes), and the short (S) isoform contains a single complete BRCT domain near its N terminus. The human MCPH1 protein domain structure is shown for comparison. Transcripts with unspliced intron 1 (indicated by dashed lines) are predicted to utilise a second translational start site, resulting in proteins with the same domain structure as MCPH1-L and/or MCPH1-S, but 47 amino acids shorter at the N terminus. (N-terminally truncated proteins not shown.) (D) In situ hybridisation of *mcpH1* transcript in wild-type embryos using clone LD43341 as probe. (a-c) *mcpH1* sense probe. (d-f) *mcpH1* antisense probe, showing that *Drosophila microcephalin* transcript is present at its highest embryonic level during syncytial stages (d). (E) Immunoblot analysis of wild-type embryos (wt) and embryos from *mcpH1^{d2/d2}* females (d2) using an affinity-purified rabbit polyclonal anti-MCPH1 antibody raised against a polypeptide at the N-terminal end of MCPH1 (AA 1-130), indicated by the antibody symbol in C. The antibody detects Microcephalin at 115 kDa in wild-type but not in *mcpH1^{d2/d2}* embryos. Loading control, cyclin B. (F) Developmental western blot of MCPH1. The 115 kDa isoform of MCPH1 is highly expressed in embryos (0-2 hour AED) and ovaries, but is present at lower levels in third instar larval brain. (G) The 115 kDa endogenous protein migrates most similarly to the short isoform. Transgenically expressed epitope tagged (Myc x6) MCPH1(L) and MCPH1(S) isoforms compared with the lower 115 kDa endogenous MCPH1 protein present in all lanes except *mcpH1^{d2/d2}* embryos. Loading control α -tubulin (α -Tub). (H) RT-PCR amplification of *mcpH1* exons 6-8 in wild-type 0- to 2-hour embryos, late embryos and testis. Primer locations indicated by arrowheads in A. The upper band corresponds to transcripts containing the unspliced intron 7, and the lower band, fully spliced exon 6-8. Control, Ribosomal protein RP49 transcript.



MCPH1 is cyclically localised during the embryonic cell cycle

Human microcephalin has been shown to associate with chromatin, and localise to DNA damage foci (Lin et al., 2005; Rai et al., 2006). As the *Drosophila* embryo presents an ideal opportunity to examine the localisation of MCPH1 during the cell cycle in vivo, we performed immunostaining on syncytial

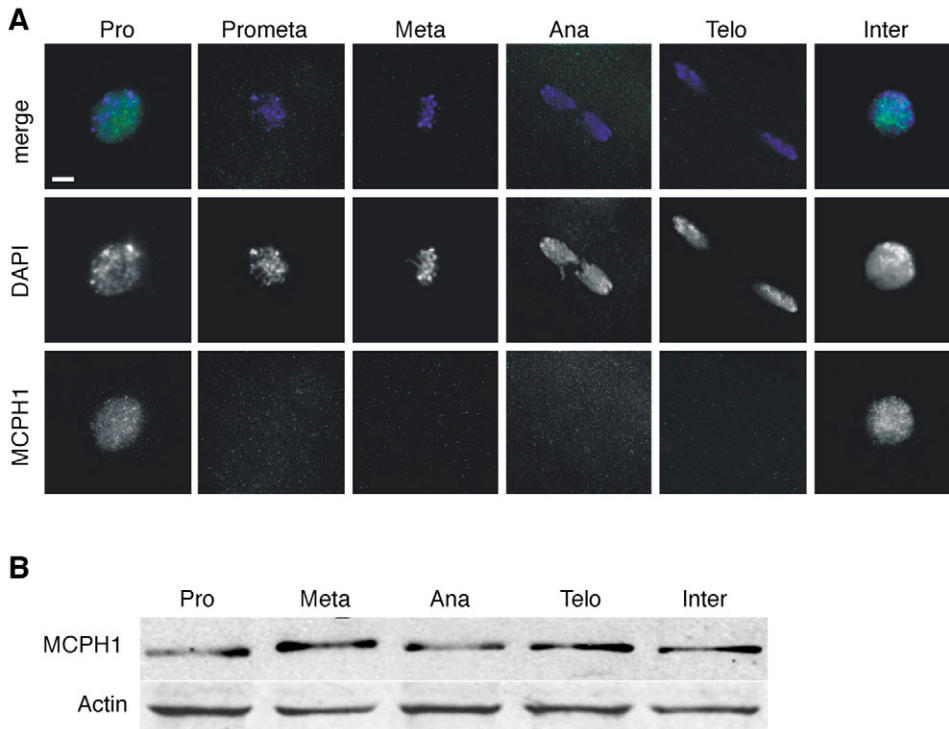


Fig. 2. MCPH1 cellular localisation in the syncytial embryo varies through the cell cycle. (A) Localisation of endogenous MCPH1 during phases of the cell cycle in syncytial blastoderm embryos. DNA (blue, DAPI); affinity purified anti-MCPH1 antibody (green). MCPH1 is detectable in prophase (Pro) and interphase (Inter) nuclei and is not detectable in prometaphase (Prometa), metaphase (Meta), anaphase (Ana) or telophase (Telo). Bar, 5 μ m. (B) Microcephalin is expressed at constant levels throughout mitosis. Methanol fixed, DAPI stained embryos from cycles 8–10 were hand sorted, and 15 embryos per mitotic stage were analysed by SDS-PAGE and immunoblotting with anti-MCPH1 antibody.

embryos with anti-MCPH1 affinity-purified polyclonal antibodies (Fig. 2A). Uniform nuclear staining was observed in interphase embryos, but was not detectable on the DNA and mitotic chromosomes from prometaphase to telophase. Nuclear staining was also present in yolk nuclei and pole cells (data not shown). Western blotting of staged cycle 8–10 embryos (Fig. 2B) revealed microcephalin to be present at a constant level throughout the cell cycle, suggesting that it was being redistributed from the nucleus rather than degraded. A small upward mobility shift was also noted at metaphase. Further investigation to identify what modifications, if any, are present at mitosis, will be useful to confirm this observation, and be of significant value in defining how microcephalin localisation at mitosis is regulated.

To confirm the finding of altered localisation in cell cycle, we cloned the L and S isoforms of *mcp1* into the pPGW vector and generated *UASP::GFP-mcp1* transgenic fly lines. Using a maternal α Tub67::Gal4VP16 driver we then performed live imaging of (overexpressed) GFP-MCPH1 in wild-type syncytial embryos to confirm that MCPH1 varies in its localisation during cell cycle (Fig. 3A,B and see Movies 1 and 2 in supplementary material). Strikingly, though the two isoforms are both nuclear during interphase, they have different localisations during mitosis. The GFP-MCPH1(L) protein is rapidly lost at the onset of mitosis, reappearing as several foci, which then expand and adopt the shape of decondensing anaphase chromosomes (Fig. 3B). By contrast, the GFP-MCPH1(S) isoform appears to localise to the centrosomes and mitotic spindle, just prior to nuclear envelope breakdown, remaining centrosomally localised until chromosome decondensation at telophase (Fig. 3A).

Notably, endogenous, as well as overexpressed chicken Mcph1 has recently been reported to localise to the centrosome, the N-terminal BRCT domain being implicated in

this localisation (Jeffers et al., 2007). A centrosomal localisation has also previously been suggested for human microcephalin (Zhong et al., 2006). Such a localisation is reminiscent of BRCA1, another BRCT domain containing protein (Hsu and White, 1998) as well as human CHK1, a direct interactant of microcephalin (Alderton et al., 2006), which negatively regulates CDK1–cyclin-B complex activity (Kramer et al., 2004).

Immunostaining of paraformaldehyde-fixed GFP-MCPH1(S) embryos confirmed that this protein is redistributed at mitosis (Fig. 3C,D,E). GFP-MCPH1(S) colocalises with DAPI staining during interphase, and is lost at the onset of chromosome condensation just after the appearance of phosphorylated histone H3 (*P*-H3). GFP-MCPH1(S) nuclear staining reappears at chromosome decondensation during telophase (Fig. 3E), closely correlating with loss of *P*-H3 staining. Localisation to the centrosome and mitotic spindle was not confirmed and could be due to limitations in detecting low levels of GFP-MCPH1 protein using anti-GFP immunostaining, or epitope masking in fixed preparations as previously described (Martinez-Campos et al., 2004; Raff et al., 2002). Further work will therefore be necessary to confirm the centrosomal localisation of MCPH1(S), which will be important in establishing its cellular functions.

mcp1 flies have a maternal effect lethal phenotype

We created deletions in the *mcp1* gene by imprecise excision of a P-element located 50 base pairs upstream of the first *mcp1* translational start site (P{GawB}NP6229, Kyoto). Two independent deletion mutants were identified by PCR screening of genomic DNA, and confirmed by sequencing the deletion breakpoints. *mcp1*^{d1} has a 1.2 kb deletion involving exons 1–3 of *mcp1*, whereas *mcp1*^{d2} is deleted for a 1.6 kb region containing exons 1–4 (Fig. 1A).

Both *mcpH1^{d1/d1}* and *mcpH1^{d2/d2}* were viable, with no morphological or behavioural phenotype evident in adult flies. In particular, we did not detect any alteration in size of the adult brain on histological examination (data not shown). While homozygous males were fertile, their female counterparts were infertile, even when crossed with wild-type males. Likewise, *mcpH1^{d1/d2}* and *mcpH1^{d1}/Df(2R) BSC39* were also viable with a maternal effect lethal phenotype.

Phase-contrast microscopy of eggs laid by *mcpH1^{d1/d1}* and *mcpH1^{d2/d2}* females only identified embryos at early developmental stages, with at most a narrow zone clearing of cytoplasm around the egg periphery without pole cell formation or cellularisation. This phenotype suggested an early defect in syncytial embryogenesis, resulting from loss of maternally contributed gene product.

mcpH1^{d1/d1} were crossed with *UASP::myc-mcpH1(S)* and *myc-mcpH1(L)* transgenic fly lines that express protein in embryos at comparable levels to endogenous protein when driven by α Tub67::Gal4VP16 (see Fig. 1G). Gal4 driven

UASP::myc-mcpH1(S) rescued the female sterile phenotype in 21.8% of embryos, whereas very few embryos (2.6%) were rescued with the *myc-mcpH1(L)* transgene (Table 1). In conjunction with the expression data, we therefore infer that loss of embryonic MCPH1(S) isoform is the cause of the *mcpH1* female sterile phenotype.

mcpH1 embryos arrest in mitosis during early syncytial cell cycles

To characterise the phenotype further we performed a time course analysis of mitotic nuclei in early embryos visualised by anti-phospho-histone H3 antibody staining (Fig. 4A). *mcpH1^{d1/d1}* embryos showed marked slowing in nuclear division compared with wild-type embryos (Fig. 4A,B). Morphologically, they also exhibited an abnormal spatial distribution of nuclei compared with wild-type embryos (Fig. 4A). Mean terminal nuclear number in mutant embryos was 11.3 (\pm 7.7; s.d.), and nuclei failed to migrate to the periphery to form the syncytial blastoderm. The terminal nuclei are in a metaphase-like state, have condensed fragmented DNA, broad mitotic spindles, and frequent separation of centrosomes from spindle poles (Fig. 4C,D). Numerous detached centrosomes were seen spread throughout the embryos indicating continued centrosomal duplication independent of nuclear division, a common feature of mitotic defects in *Drosophila* (Freeman et al., 1986; Raff and Glover, 1988). Monopolar (Fig. 4E) and multipolar spindles (Fig. 4F) as well as acentrosomal broad-based spindles (Fig. 4G) could be observed in the terminally arrested embryos. In view of the phenotype we therefore concluded that MCPH1(S) is essential for mitosis during early embryogenesis.

Asynchrony of nuclear and centrosome cycles in *mcpH1* embryos

Multiple perturbations, such as blocked DNA replication (Raff and Glover, 1988), loss of centrosomal components (Megraw et al., 1999; Vaizel-Ohayon and Schejter, 1999), extensive DNA damage, and failure to degrade cyclins (Swan et al., 2005) can result in a metaphase-like state with detached centrosomes in the syncytial embryo. To understand further the underlying mechanism of the phenotype, we analysed mitosis by immunostaining of embryos 0–30 minutes after egg deposition (AED). We found morphological abnormalities apparent from cycle 1 in *mcpH1* mutant embryos (Fig. 5B) compared to control embryos (Fig. 5A).

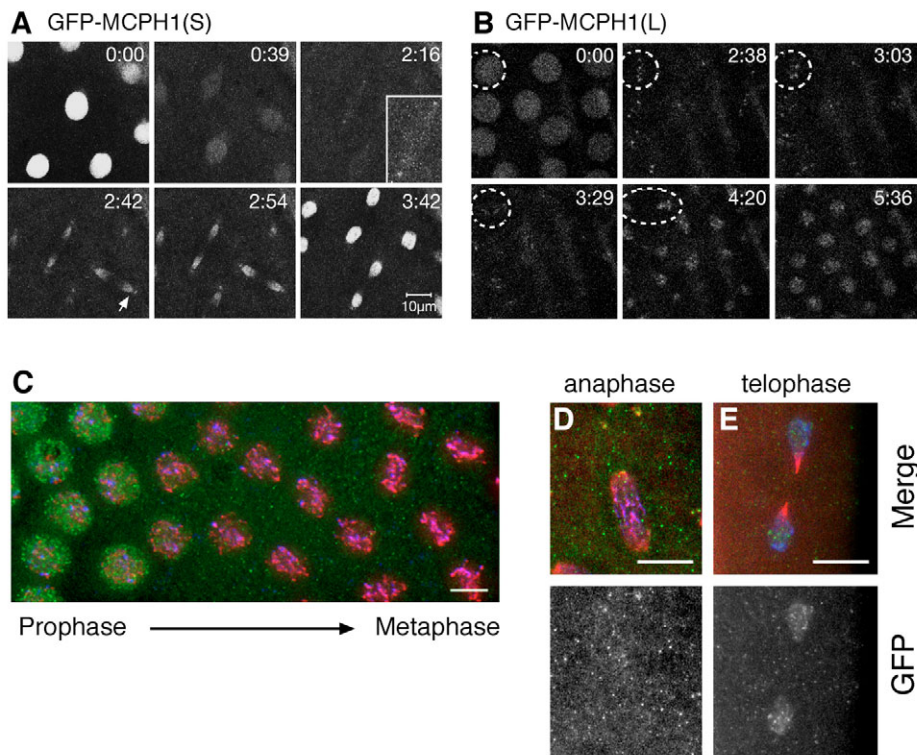


Fig. 3. GFP-MCPH1(S) and GFP-MCPH1(L) have different subcellular localisations during mitosis. (A,B), GFP-MCPH1(S) and GFP-MCPH1(L) isoforms expressed in blastoderm stage embryos followed from interphase to subsequent interphase, show different localisations during mitosis. Time in minutes is shown at the top right of each panel. Bar, 10 μ m. (A) After nuclear envelope breakdown GFP-MCPH1(S) is localised at the centrosomes, and faintly on the spindle (inset t=2:16, time in minutes:seconds). At later stages of mitosis, increased fluorescence is seen at the spindle poles, either representing increased protein at the spindle poles, or accumulation on decondensing chromosomes (t=2:42, arrow). (B) GFP-MCPH1(L) is localised to the interphase nucleus, and this localisation is lost at the onset of mitosis. Several foci of GFP-MCPH1(L) then appear (t=2:38, representative nucleus, circled). These foci then appear to separate (t=3:03), and the fluorescent signal then expands to become decondensing. (C) In fixed blastoderm embryos nuclear GFP-MCPH1(S) staining is lost during prophase as DNA becomes histone H3 phosphorylated. (D) Anaphase and (E) telophase: GFP-MCPH1(S) reappears in decondensing telophase nuclei with loss of phosphoH3 staining. DNA (DAPI, blue), anti-GFP antibody (green), anti-phospho-histone H3 (red) in C,D and E. Bar, 10 μ m.

Table 1. Rescue of mutant phenotype

Maternal genotype	No. hatching	Total embryos	% Hatched
Oregon (WT)	269	319	84.3
<i>mcp1^{d1/d1}; UAS::Myc-mcp1^{Short}/αTub67C::GalVP16</i>	67	308	21.8
<i>mcp1^{d1/d1}; UAS::Myc-mcp1^{Long}/αTub67C::GalVP16</i>	7	267	2.6
<i>mcp1^{d1/d1}; UAS::Myc-mcp1^{Long}</i>	0	202	0.0
<i>mcp1^{d1/d1}; UAS::Myc-mcp1^{Short}</i>	0	201	0.0
<i>mcp1^{d1/d1}; αTub67C::GalVP16</i>	0	203	0.0
<i>mcp1^{d1/d1}</i>	0	343	0.0

Virgin females of the genotypes described were mated to Oregon males and eggs were collected at 22°C and scored for hatching.

The most striking abnormalities involved the centrosomes. Centrosomin signals were duplicated as early as prophase (Fig. 5C) suggesting the occurrence of premature separation of centrosomes (i.e. of centrioles and pericentriolar material). The occasional presence of additional centrosomin foci (prophase, Fig. 5B), also raised the possibility of the alternative explanation of centrosome overduplication.

Additionally, detachment of centrosomes from the spindle pole(s) was also frequently seen at metaphase 1 (26%, $n=19$) and onwards (Fig. 5B, anaphase). Increased α -tubulin localisation was also noted at the centrosomes, and astral microtubules, though fainter, were present. In cycle 1, tripolar and unipolar metaphase figures were also seen, presumably the consequence of centrosome separation and detachment. Similar abnormalities were seen in later cycles (Fig. 4E,F,G), and, from cycle 2 onwards, asynchronous mitotic divisions could also be observed.

Other, non-centrosomal abnormalities were also present. At pronuclear fusion and prophase in mutant embryos, chromosomes may be less compact than in wild-type embryos, relative to progress made in centrosome positioning and spindle formation in the respective embryos (Fig. 5A,B). However, at metaphase, mutant chromosomes were condensed to a similar extent as in wild-type embryos. Mitotic spindles at metaphase were irregular and less well formed in *mcp1* mutants compared with simultaneously fixed wild-type embryos. During anaphase, there was occasional appearance of chromosome lagging, perhaps due to the less robust mitotic spindles. At telophase there was a less well formed midbody.

To obtain an accurate description of mitotic progression in *mcp1* embryos, we quantified the relative frequency of mitotic phases in 0-30 minute AED embryos (Fig. 5D). We found that there was a disproportionate accumulation of *mcp1* embryos in cycle 1 (29.3% *mcp1*, 12.0% Oregon, χ^2 -test $P<0.001$, $n=601$, $n=656$, respectively). In particular many more *mcp1* embryos were in prophase 1 (9.3% *mcp1*, 4.6% Oregon, χ^2 -test $P<0.001$) and metaphase 1 (12.1% *mcp1*, 3.5% Oregon, χ^2 -test $P<0.001$).

Given that the short isoform of Microcephalin may localise to the centrosome during mitosis, we also investigated whether it is required for assembly of known components of the mitotic spindle poles and centrosomes. Asp, Cnn, and γ -tubulin all localised appropriately and at comparable levels to those in wild-type embryos (Fig. 4D,H,I). Thus we found no evidence to suggest a role for MCPH1 in the assembly of structural elements of the centrosome and/or spindle poles.

Inhibitory phosphorylation of Cdk1 is reduced in *mcp1* embryos

To investigate whether perturbation of key regulatory cell cycle proteins could explain the observed slowing of the nuclear

cycle, we performed immunoblotting on 0- to 1-hour AED *mcp1* embryos (Fig. 6). There was no accumulation of cyclins as has previously been reported as a cause of mitotic arrest in *remnant* mutant embryos (Swan et al., 2005), neither were there any abnormalities in total Cdk1 or Chk1 (also known as Grapes; Grp) protein levels. Reduced inhibitory phosphorylation on tyrosine 15 of Cdk1, similar to that seen in human patient cell lines (Alderton et al., 2006) was observed.

Discussion

The role of *mcp1* in the cell cycle

We report here that *Drosophila* MCPH1 localisation is mitotically regulated and that *mcp1* mutant flies have a maternal effect lethal phenotype, as a result of mitotic arrest occurring in early syncytial cell cycles. We find that a short isoform of MCPH1 lacking C-terminal BRCT domains rescues this phenotype, indicating that this protein has an essential role in these embryonic cell cycles. GFP-MCPH1(S) localises to the centrosomes during mitosis, suggesting that it might have centrosomally related functions, relevant to the primary microcephaly phenotype. No centrosomal or spindle abnormalities during neuroblast mitosis have been observed in the larval brains of *mcp1* mutants and the asymmetric determinants Inscuteable and Miranda also appeared to be appropriately localised (B.V. and A.P.J., unpublished data). Therefore, the centrosomal abnormalities appear to be specific to the early embryonic cell cycles. These data, along with the slowed rate of nuclear division in embryos (Fig. 4A), present from cycle 1 (Fig. 5D), lead us to conclude that the embryonic phenotype is the result of nuclear division cycle being slowed relative to the centrosome cycle. Additional centrosomes are consequently generated, perturbing subsequent nuclear divisions, leading to nuclear fragmentation and terminal mitotic arrest or catastrophe. In the syncytial embryo even a small reduction in nuclear division rate may have major effects, as cell cycle is very rapid, comprising rapid synchronous S and M phases without intervening G1 and G2 phases (Edgar et al., 1994). A subtle effect on cell division timing in all cells could therefore be sufficient to explain the essential requirement for MCPH1 in the syncytial embryos, but not in other cell cycles. Alternatively, MCPH1, and in particular the S isoform may have a specialised function, which is important for these cycles.

What causes the nuclear cycle to slow? The nuclear cycle is retarded prior to metaphase in cycle 1 (Fig. 5D). This might be because of prolonged mitotic entry, similar to the perturbed cell cycle regulation observed in human cells where there is an extended prophase-like state of "premature chromosome condensation" (Alderton et al., 2006; Trimborn et al., 2004).

Fig. 4. *mcpH1* has an early maternal effect lethal phenotype with cell cycle arrest in a metaphase-like state.

(A) Time course of nuclear division in wild-type and *mcpH1^{d1/d1}* embryos. Mitotic nuclei are stained with phosphoH3 antibody. *mcpH1^{d1/d1}* embryos have a reduced number of nuclei, which become non-uniform in distribution and never migrate to the surface. By 2 hours, *mcpH1^{d1/d1}* embryos begin to degenerate, exhibiting shape irregularities and disintegration of the yolk. (B) Number of nuclei per embryo. Mean number of nuclei is reduced in *mcpH1* mutants at all time points (AED at 25°C), indicating that nuclear division is markedly slowed. Number of nuclei in mutants is not 2n in the majority of embryos, suggesting loss of mitotic synchrony. Error bars, standard deviation. The numbers of wild-type nuclei plotted from 70 to 135 minutes are extrapolated from published data (Sullivan et al., 2000). (C-G) Terminal phenotype of *mcpH1^{d2/d2}* embryos. DNA (DAPI, blue), microtubules (α -tubulin, green), centrosomes [Centrosomin (Cnn), red]. (C) *mcpH1^{d2/d2}* embryo: nuclei in a metaphase-like state, with multiple free centrosomes. (D) Detail from embryo shown in C (boxed). (E) Monopolar, monoastral, and (F) multipolar spindles are also seen. (G) Fragments of DNA also become distributed onto the acentrosomal anastral spindle. Asp localises on spindle poles (H) and gamma-tubulin is present at the centrosome (I) in mutant embryos. DNA (DAPI, blue), microtubules (α -tubulin, green), Asp (H, red) or γ -tubulin (I, red). Bars, (C) 50 μ m, (D) 10 μ m, (E,F,G) 10 μ m, (H,I) 8 μ m.

(A) Time course of nuclear division in wild-type and *mcpH1^{d1/d1}* embryos. Mitotic nuclei are stained with phosphoH3 antibody. *mcpH1^{d1/d1}* embryos have a reduced number of nuclei, which become non-uniform in distribution and never migrate to the surface. By 2 hours, *mcpH1^{d1/d1}* embryos begin to degenerate, exhibiting shape irregularities and disintegration of the yolk. (B) Number of nuclei per embryo. Mean number of nuclei is reduced in *mcpH1* mutants at all time points (AED at 25°C), indicating that nuclear division is markedly slowed. Number of nuclei in mutants is not 2n in the majority of embryos, suggesting loss of mitotic synchrony. Error bars, standard deviation. The numbers of wild-type nuclei plotted from 70 to 135 minutes are extrapolated from published data (Sullivan et al., 2000). (C-G) Terminal phenotype of *mcpH1^{d2/d2}* embryos. DNA (DAPI, blue), microtubules (α -tubulin, green), centrosomes [Centrosomin (Cnn), red]. (C) *mcpH1^{d2/d2}* embryo: nuclei in a metaphase-like state, with multiple free centrosomes. (D) Detail from embryo shown in C (boxed). (E) Monopolar, monoastral, and (F) multipolar spindles are also seen. (G) Fragments of DNA also become distributed onto the acentrosomal anastral spindle. Asp localises on spindle poles (H) and gamma-tubulin is present at the centrosome (I) in mutant embryos. DNA (DAPI, blue), microtubules (α -tubulin, green), Asp (H, red) or γ -tubulin (I, red). Bars, (C) 50 μ m, (D) 10 μ m, (E,F,G) 10 μ m, (H,I) 8 μ m.

(C) *mcpH1^{d2/d2}* embryo: nuclei in a metaphase-like state, with multiple free centrosomes. (D) Detail from embryo shown in C (boxed). (E) Monopolar, monoastral, and (F) multipolar spindles are also seen. (G) Fragments of DNA also become distributed onto the acentrosomal anastral spindle. Asp localises on spindle poles (H) and gamma-tubulin is present at the centrosome (I) in mutant embryos. DNA (DAPI, blue), microtubules (α -tubulin, green), Asp (H, red) or γ -tubulin (I, red). Bars, (C) 50 μ m, (D) 10 μ m, (E,F,G) 10 μ m, (H,I) 8 μ m.

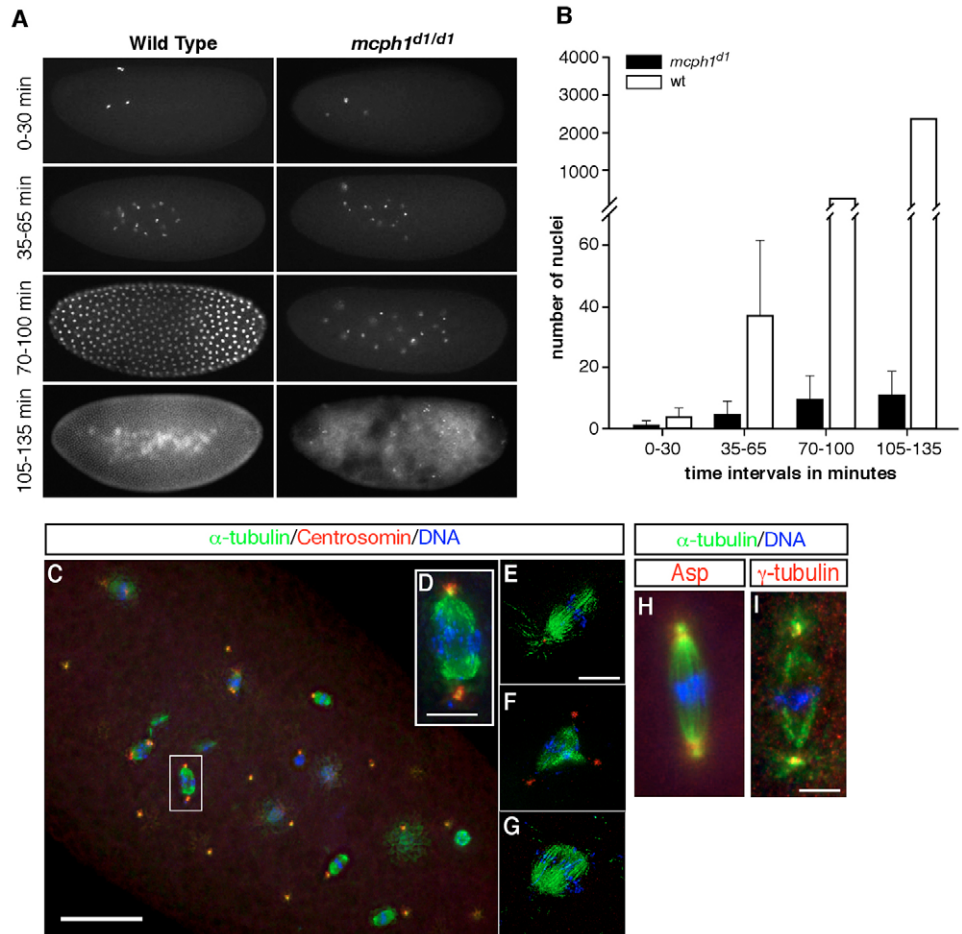
(C) *mcpH1^{d2/d2}* embryo: nuclei in a metaphase-like state, with multiple free centrosomes. (D) Detail from embryo shown in C (boxed). (E) Monopolar, monoastral, and (F) multipolar spindles are also seen. (G) Fragments of DNA also become distributed onto the acentrosomal anastral spindle. Asp localises on spindle poles (H) and gamma-tubulin is present at the centrosome (I) in mutant embryos. DNA (DAPI, blue), microtubules (α -tubulin, green), Asp (H, red) or γ -tubulin (I, red). Bars, (C) 50 μ m, (D) 10 μ m, (E,F,G) 10 μ m, (H,I) 8 μ m.

In this view, the loss of MCPH1 could affect the coordination of chromosome condensation with the rest of cell cycle entry. The larger, less compacted nuclei seen at pronuclear fusion and prophase could suggest that chromosome compaction or condensation might be delayed relative to other events at mitotic entry. However, live imaging of mutant embryos would be required to confirm this, but has not been technically possible in such early embryos. Immunofluorescence and live imaging studies of GFP-tagged and endogenous MCPH1 protein in wild-type embryos revealed an inverse correlation of MCPH1 localisation with mitotically condensed chromosomes, consistent with a role for this chromatin-associated protein (Lin et al., 2005) in maintaining decondensed chromosomes (Fig. 3C,D,E). Reduced Cdk1 inhibitory phosphorylation (*P*-Cdk1^{tyr15}) has been observed in S and G2 phases of human MCPH1 cell lines (Alderton et al., 2006), and suggested to underlie the early onset of chromosome condensation in human cells relative to other mitotic events. *P*-Cdk1^{tyr15} is also reduced in *mcpH1^{d2/d2}* embryos (Fig. 6), which could explain the asynchrony of centrosomal and nuclear events observed. However, we cannot rule out that this is a secondary consequence of mitotic arrest in these embryos.

A second possibility is that S phase is prolonged in *mcpH1* embryos. Embryos in which DNA synthesis is blocked by

aphidicolin injection, have similarly slowed cell cycles, with particularly slowed (paradoxically) M phase (Raff and Glover, 1988). Such embryos still undergo cycles of chromosome condensation and decondensation and exhibit centrosome overduplication. In *Drosophila* the ATR/Chk1 pathway prevents premature mitotic entry while S phase is still ongoing, only becoming developmentally required at mid-blastula transition when both ATR and Chk1 become essential (Sibon et al., 1999; Su et al., 1999). The *mcpH1* phenotype, however, is manifest much earlier than either of these mutants, inconsistent with its being initiated by defective ATR/Chk1 signalling. Additionally, though RNAi experiments have suggested that human microcephalin might transcriptionally regulate CHK1 (Lin et al., 2005; Xu et al., 2004), Chk1 protein levels are unaltered in *mcpH1* embryos (Fig. 6). Rather it seems more likely, that there is a separate function for *Drosophila* MCPH1 in cell cycle regulation, independent of its downstream role in ATR/Chk1 signalling, as has been previously concluded from analysis of human MCPH1 patient cell lines (Alderton et al., 2006).

Nuclear cell cycle can also be slowed if cyclins fail to degrade, and is the cause of mitotic arrest in the *Cks30A* mutant (Swan et al., 2005). A global accumulation of Cyclin A, B or



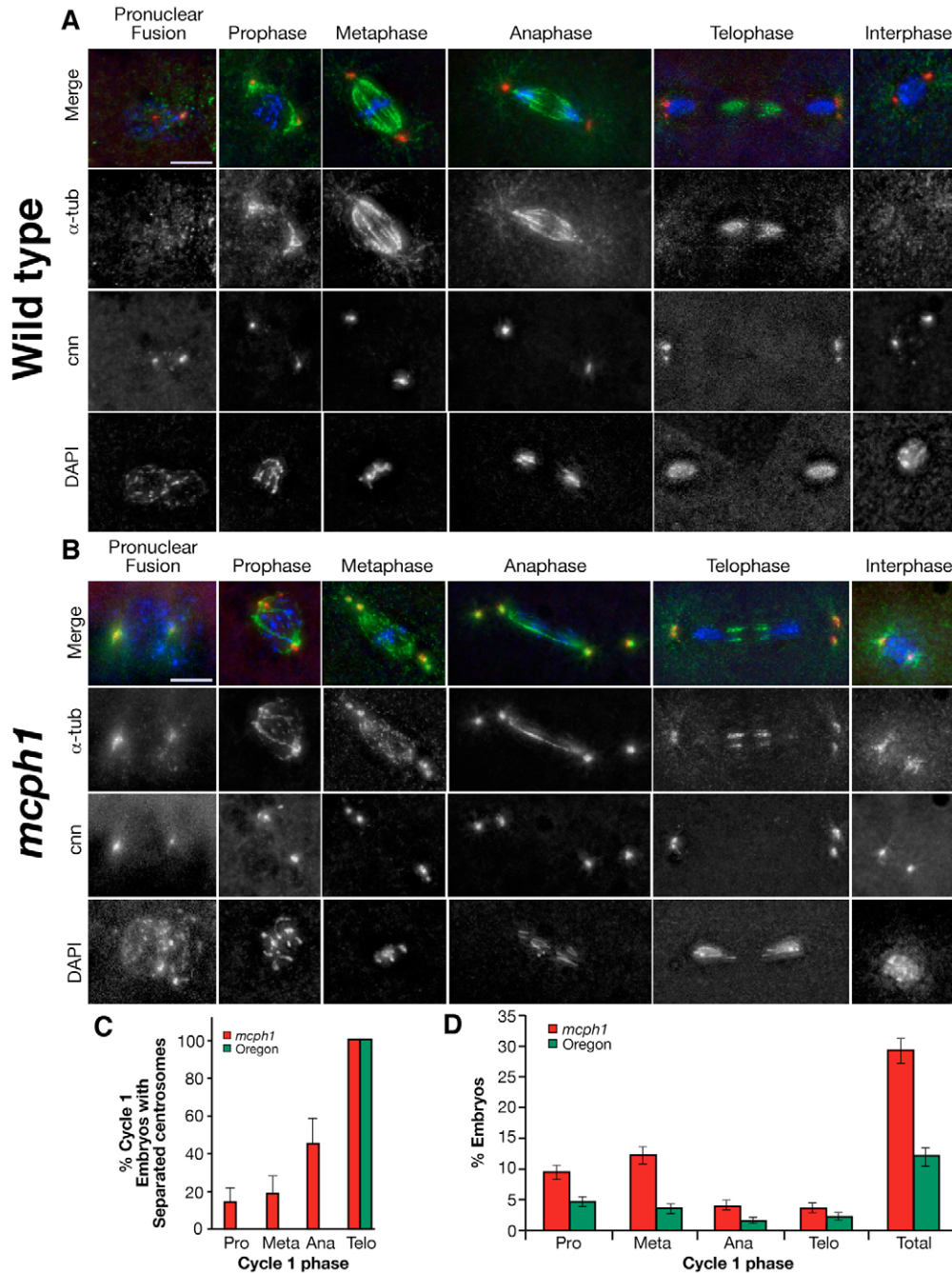


Fig. 5. Centrosomal abnormalities are present from the first mitotic cycle. (A) Mitosis in cycle 1 in wild-type Oregon embryos. DNA (DAPI, blue), microtubules (α -tubulin, green), centrosomes (Cnn, red). Centrosome separation occurs at telophase in wild-type embryos. (B) Cycle 1 mitosis in *mcp1*^{d2/d2} embryos. Nuclear compaction is less advanced at pronuclear fusion and prophase in mutant embryos (larger nuclear diameter than in wild type). Duplication of Centrosomin signal is also apparent from prophase, much earlier than in wild-type embryos. By metaphase, centrosomes are tandemly duplicated along the axis of the spindle, rather than side by side. Centrosome detachment also occurs, and increased α -tubulin is seen at the centrosome, compared to that in wild-type embryos. The mitotic spindle is irregular and less substantial. Bar, 10 μ m. (C) Centrosomal separation occurs earlier in *mcp1*^{d2/d2} embryos than wild-type Oregon cycle 1 embryos. $n=66$ *mcp1*, $n=22$ Oregon. (D) Proportion of cycle 1 embryos by mitotic stage, from 0-30 minute AED embryos collections of wild-type and *mcp1*^{d2/d2} females. There is an excess of *mcp1*^{d2/d2} embryos at prophase and metaphase in cycle 1 ($P<0.001$). Error bars, standard error. *mcp1*, total embryos scored $n=601$, unfertilised $n=125$, meiosis $n=66$, cycle 1 $n=179$, cycle 2 and later $n=231$ (38.44%). Oregon, total embryos scored $n=656$, unfertilised $n=81$, meiosis $n=55$, cycle 1 $n=179$, cycle 2 and later $n=418$ (63.72%).

B3 does not, however, occur in *mcp1*^{d2/d2} embryos. (Fig. 6; K.B. and A.P.J., unpublished). In the embryo, cell cycle progression is regulated by localised Cyclin B degradation on the mitotic spindle (Huang and Raff, 1999). Degradation occurs from spindle poles inwards, and appears to be mediated by the centrosome (Wakefield et al., 2000). Therefore, both the poorly formed mitotic spindles and detachment of centrosomes observed in *mcp1* embryos could also delay progression in the nuclear cycle through inhibition of local Cyclin B degradation. Consistent with this, Cyclin B immunostaining was observed on terminally arrested mutant nuclei (data not shown).

In summary, any of these abnormalities – localised failure in cyclin degradation, perturbed regulation of chromosome

condensation, or prolonged DNA synthesis – could account for the *mcp1* maternal effect lethal phenotype. Each would delay mitotic entry through slowing the nuclear cycle while the centrosomal cycle would continue unchecked, resulting in premature separation and detachment of centrosomes. Lost connections of centrosomes with spindles would then delay mitosis further, through impaired Cyclin B degradation, and insubstantial mitotic spindle formation. Further centrosome-nuclear incoordination subsequently would result in mitotic catastrophe and arrested embryo development.

An alternative, more speculative, interpretation is that the *mcp1* phenotype has a centrosomal aetiology. Firstly, there is a correlation between phenotypic rescue with MCPH1(S), and the apparent centrosomal localisation of this isoform during

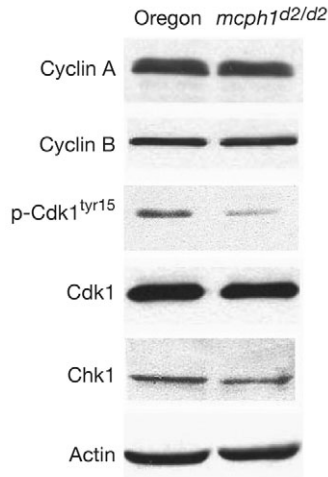


Fig. 6. *mcp1* mutant embryos have reduced inhibitory phosphorylation of Cdk1, and normal Cyclin protein levels. Immunoblot analysis of wild-type embryos and *mcp1*^{d2/d2} embryos 0–1 hour AED. Immunoblotted embryo extracts for Cyclin A, Cyclin B, Cdk1 phospho-tyrosine 15 (p-Cdk1^{Tyr15}), Cdk1, Chk1, and Actin as a loading control. *mcp1*^{d2/d2} embryos have a reduced level of inhibitory Cdk1 phosphorylation compared to wild-type embryos, whereas other cell cycle proteins are apparently present at normal levels.

mitosis. Furthermore, the early separation of centrosomes observed could reflect a requirement for microcephalin in maintaining the two centrioles together during mitosis and attachment of centrosomes to the spindle poles. Early separation and centrosome detachment would result in failure of localised Cyclin B degradation (Wakefield et al., 2000) and a consequently delayed nuclear cycle, culminating in mitotic catastrophe and arrested embryo development.

mcp1 as a model for primary microcephaly

The cerebral cortex is reduced to a third of normal volume in primary microcephaly. The marked reduction in neural cell number is presumed to be caused by inefficient neurogenic mitosis (Woods et al., 2005). Primary microcephaly brain size is similar to that of early hominids, and the Darwinian adaptive evolutionary changes observed in primate microcephalin suggest that changes in this gene could have contributed to the evolutionary expansion of the human brain (Evans et al., 2004). Given the evolutionary scaling of the brain (Northcutt and Kaas, 1995), it is unsurprising that the invertebrate *mcp1* fly brain is not grossly reduced in size. Nevertheless, our finding here that *mcp1* is required for mitosis in the *Drosophila* embryo is pertinent to understanding the disease phenotype. Although a complete elucidation of the cell cycle function of MCPH1 will be necessary for unravelling its role in brain development and evolution, our finding here that the short isoform, lacking C-terminal BRCT domains, functions in coordinating mitosis is likely to be relevant to the pathogenesis of primary microcephaly. Moreover, as BRCT domains are important in phosphoserine/threonine-dependent protein binding (Manke et al., 2003; Yu et al., 2003) we would predict that this protein lacking functional C-terminal tandem BRCT domains will have significantly different functions from the full-length protein. In this context, it is notable that a recent

analysis of MCPH1 in DT40 cells has demonstrated that the C-terminal BRCT domains are required for microcephalin localisation at ionising radiation-induced DNA damage repair foci (Jeffers et al., 2007). The fly, therefore, provides an ideal opportunity for analysis of the role of microcephalin in DNA damage repair, having physiological isoforms of microcephalin, with and without these C-terminal BRCT domains.

Two of the other primary microcephaly homologue mutants (*asp*, *cnn*) also exhibit maternal effect lethal phenotypes with mitotic arrest and free centrosomes (Gonzalez et al., 1990; Megraw et al., 1999; Vaizel-Ohayon and Schejter, 1999) and are therefore also required for mitosis in the early fly embryo. Furthermore, the mitotic centrosomal localisation of GFP-MCPH1(S) is intriguing, as it suggests that Microcephalin could co-localise with the other primary microcephaly proteins during mitosis. In contrast to the nuclear localisation generally reported for Microcephalin (Lin et al., 2005; Xu et al., 2004), all other primary microcephaly proteins, ASPM, CDK5RAP2 and CENPJ, and their *Drosophila* homologues (Asp, Cnn and Sas-4, respectively) are centrosomally localised (Basto et al., 2006; Bond et al., 2002; Bond et al., 2005; do Carmo Avides and Glover, 1999; Megraw et al., 1999). Therefore *Drosophila* MCPH1 could still act in the same biochemical pathway as other primary microcephaly orthologs.

Conclusions

In summary, we have shown that MCPH1 is a mitotically regulated protein, which co-localises with decondensed chromosomes, with a short isoform, MCPH1(S), localising to the centrosome and spindle during mitosis. MCPH1(S) is essential for the early rapid syncytial nuclear divisions, where it is required to co-ordinate centrosome and nuclear division cycles, prior to the physiological requirement for ATR-Chk1 signalling in the blastoderm embryo. The *mcp1* fly therefore provides a relevant model for further genetic and biochemical characterisation of microcephalin's role in cell cycle regulation during development. Given that MCPH1 may co-localise with other primary microcephaly proteins at the spindle and centrosome during mitosis, this model also provides the opportunity to examine whether they may act in a common developmental and cellular pathway underlying the human phenotype.

Materials and Methods

Stocks

Stocks were maintained on standard cornmeal *Drosophila* medium at 25°C. Wild-type flies were of Oregon^R strain. *mcp1* deletion alleles were generated by imprecise excision of the isogenised P-element insertion line P{GawB}NP6229 (Kyoto), and maintained on a CyO, P{ActGFP}JMR1 balancer.

MCPH1 antibody generation and purification

A DNA fragment, encoding the first 130 amino acids of MCPH1 was cloned into pGEX-6P1 (Amersham) and used to generate a N-terminal GST-fusion protein. The *mcp1*(S) transcript was excised from the LD43341 clone (DGRC, pOT2 vector) using *Nco*I and *Xho*I restriction sites. The *Nco*I and *Xho*I fragment was then directionally cloned (after filling in of the *Nco*I site) into *Sma*I, *Xho*I sites in the pGEX-6P1 vector to create pGEX6P1-MCPH1(S). A *Bgl*II-*Not*I digest was then performed to remove the 3' end of this transcript, and after infilling of overhangs, the vector was religated to generate the final pGEX6P1-MCPH1 (1–130aa) construct. The vector was transfected into *E. coli* Rosetta (Novagen) and soluble GST fusion protein generated using standard methods (GST Gene Fusion Manual; Amersham Biosciences). After cleavage of the GST tag using Precision Protease (Amersham), the MCPH1(1–130aa) polypeptide was then used to generate polyclonal rabbit antibodies (Eurogentec). Antibodies were affinity purified from

sera using the antigen coupled to HiTrap NHS-activated HP columns (GE Healthcare) following the manufacturer's protocol.

Plasmids

UASP-Myc-mcph1^{Long}, *UASP-Myc-mcph1^{Short}*, *UASP-mcph1^{Long}* and *UASP-EGFP-mcph1^{Short}* constructs were generated using the Gateway system (Invitrogen). *mcph1* full length and *CG8981* coding sequences were cloned by PCR amplification and recombination of the PCR products into pENTRY 221 (Invitrogen) using the following primers:

Forward primer for both isoforms (5'-GGGGACAAGTTTGTACAAAAAGCAGGCTTACCATGGACAAGTTTCTGTGTGCGc-3'), Long isoform reverse primer (5'-GGGGACCACTTTGTACAAGAAAGCTGGGTCTATTGTCCAGCACAAACGGTGGGA-3'), Short isoform reverse primer (5'-GGGGACCACTTTGTACAAGAAAGCTGGGTCTACTCCGTCGTATTACCAACCTTG-3'). The plasmid clone LD43341 (DGRC) and pGEX6P1-mcph1(L) were used as the PCR template for mcph1(S) and mcph1(L).

pGEX6P1-mcph1(L) was generated by utilising an internal *NheI* restriction site within the *mcph1* sequence of the pGEX6P1-MCPH1(S) plasmid to insert the longer alternative 3' transcript end: primers D8F, CATCGAGCTCGGTGCAGAAAG and D8R, GGTACTCTGTGTGCTAGC were used to amplify the 3' end of *mcph1(L)* transcript from testis cDNA, and were cloned into pGEM-Teasy. From this a *NheI* and *SpeI* restriction fragment was then subcloned into pGEX6P1-mcph1(S), that had been digested with *XhoI* (filled in) and *NheI* to remove the 3' end of *mcph1(S)*.

The resulting mcph1(S) and mcph1(L) pDonor vectors were then recombined into UASP N-terminal Myc and N-terminal EGFP destination vectors (pPMW and pPGW; Terence Murphy, Carnegie Institute, USA). Transgenic lines were generated by standard germ line transformation. Transgenes were expressed in embryos using the alphaTub67C::Gal4-VP16 maternal driver (w[*]; P{w[*+mC]=matalpha4-GAL-VP16}V2H, Bloomington #7062). All strains, unless otherwise stated were obtained from the Bloomington stock center. Others genotypes were generated by standard *Drosophila* genetics.

Live imaging analysis

Embryos were processed as described previously (Davis, 2000). Embryos were imaged by time-lapse confocal microscopy using a Zeiss LSM 510 Meta scanning confocal system mounted on a Zeiss Axiophot II microscope with a ×63 objective Plan-Apochromat (1.4 NA). Three focal planes spaced by 0.5 μm were acquired every 12–15 seconds. All images shown are maximum intensity projections and were processed with Zeiss LSM 510 Images Browser (Zeiss).

Embryos fixation and immunostaining

Embryos from timed collections were dechorionated in 50% sodium hypochlorite, fixed in a two phase mixture of (1) heptane and methanol (1:1) containing 10 mM EGTA for α-tubulin, γ-tubulin, Asp and Cnn immunostaining; (2) heptane and 37% formaldehyde (1:1) for 5 minutes at room temperature for the detection of phosphohistone H3, GFP and MCPH1. Embryos were devitellinised in methanol, rehydrated in PBT (phosphate-buffered saline plus 0.1% Triton X-100) at room temperature and blocked in PBTA (PBS, 1% BSA and 0.1% Triton X-100) for 1 hour at room temperature. Primary antibody incubations were carried out overnight at 4°C. Subsequently, embryos were washed for 1 hour at room temperature in PBTA, and incubated for 1 hour with Alexa Fluor 488, Alexa Fluor 568 and 594 secondary antibodies (Molecular Probes) at 2 μg/ml in PBTA, washed for 1 hour at room temperature in PBT then mounted in Vectashield (Vector Labs) with DAPI at 5 μg/ml. Primary antibodies, rat anti-α-tubulin (1:10; YL1/2, Serotec), mouse anti-γ-tubulin (1:100; GTU-88, Sigma), mouse anti-GFP (1/200 JL-8, Clontech), rabbit anti-phospho-histone H3 (1:500; Upstate Biotechnology), rabbit anti-Cnn (1:100; a gift from T. Kaufman), rabbit anti-MCPH1 (1/10, this study), rabbit anti-Asp (1/25; a gift from D. Glover, Cambridge University, UK).

Fluorescence imaging

Single images or Z-series were collected on an Axiovert 200 microscope (Zeiss) with a 63× Plan-APOCHROMAT (1.4 NA) objective using IPLab 4.0 image capture software. Deconvolution was performed using Autoquant X (MediaCybernetics, Bethesda, MA).

In situ hybridisation

0- to 16-hour embryos were collected on apple juice agar plates, dechorionated in 100% household bleach, devitellinised and fixed as described previously (Lehmann and Tautz, 1994). Embryos were fixed in 3.7% paraformaldehyde in PBS. Digoxigenin-labeled antisense and sense RNA probes corresponding to the GDC.11-D11 (LD43341, BDGP) embryonic cDNA clone sequence were prepared by in vitro transcription using digoxigenin-11-UTP labelling kit (Roche) with T7 and SP6 RNA polymerase respectively. Hybridisation to the fixed embryos was performed as described previously (Lehmann and Tautz, 1994).

Immunoblotting

Embryos were collected and dechorionated in 50% sodium hypochlorite as above. Dechorionated embryos were washed twice in 0.7% saline, 0.1% Triton X-100 and

subsequently three times in embryo sample buffer [50 mM Tris-HCl pH 8.0; 150 mM NaCl; 0.5% Triton X-100; 1 mM EGTA, and protease inhibitor cocktail (Roche)]. Embryos were homogenised in 1.5 ml tubes in 1 volume embryo sample buffer using a pellet pestle homogeniser (Anachem, Luton, UK). The homogenate was cleared by repeated centrifugation for 10 minutes at 4°C at 13,000 g and stored at -20°C. Extracts were separated by SDS-PAGE and transferred to Hybond ECL membrane (GE Healthcare, Chalfont St Giles, UK). Primary antibodies used: rabbit anti-MCPH1 (this study, 1:1000), mouse anti-myc (clone 9B11, 1:2500, Cell Signaling), mouse anti-α-tubulin (clone B-152, 1/10000, Sigma), rabbit anti-cyclin B (Rb270, 1/3000, a gift from D. Glover), rabbit anti-cyclin B (Rb271, 1/3000, a gift from D. Glover), mouse anti-actin antibody (clone AC-40, 1:1000, Sigma), rabbit anti-chk1 (grp,1:500, a gift from T. T. Su, University of Colorado, Boulder, CO), rabbit anti-phosphoTyr15-cdc2 (*P-Cdk1^{Yr15}*, dilution 1:1000, Cell Signaling), mouse anti-cdk1 (PSTAIR, 1:5000, Sigma). Secondary antibodies (horseradish peroxidase labelled, anti-rabbit, Sigma; anti-mouse, DAKO) were used at a 1:2500 dilution. Chemiluminescence detection was performed using ECL western blotting substrate or ECL Advance detection system (GE Healthcare). For ECL Advance system all primary antibody concentrations were decreased tenfold and secondary antibodies were used at 1:200,000.

Extracts from defined mitotic stages were prepared as previously described (Su, 2000) from syncytial embryos at division cycles 8–10. DNA was visualised by DAPI staining and for each cell cycle stage 15 hand selected embryos were electrophoresed and blotted.

RT-PCR

RNA was isolated using Tri reagent (Sigma) according to manufacturer's instructions. Reverse transcription was performed using random primers and AMV reverse transcriptase (Roche). PCR was carried out using control primers for *RP49* (Gabler et al., 2005): rp-49-F, TGTCCTTCCAGCTTCAAGATGACCATC and rp-49-R, CTTGGGCTTGCCGCAATTTGTG. *mcph1* primers were, exon 6: F, GCCATTAACCAATAAGCCATCGG, and exon 8: R, CTCATAGGGCTCTTCATTGATCC. Thirty-two cycles of PCR were performed with an annealing temperature of 57°C.

RT-PCR primers for the *mcph1(L)* transcript fragments (supplementary material Fig. S1) were respectively:

Fragment 1F/R: D4F, GCAATAAGGACGCCAGAGTG and D4R, ACGCCCTCAGAGCGATTGTC, Fragment 2F/R: D5F, ATCATCACGATGGAAGAACGCA and D5R, CATTCTCGTATCCGTTGCAGGA, Fragment 3F/R: D6F, GCCAGCCACAACTACTCAA and D6R, CCTGGCCCTCGGAGCTAAGTT, Fragment 4F/R: D7F, TGATGGACATAAGTTCTCTCTCG and D7R, TTGGATCCAGCCGATGCGG, Fragment 5F/R: D8F, CATCGAGCTCGGTGCAGAAG and D8R, GGTACTCTGTGTCTAGC.

We thank Vicky Thomas-McArthur and Debbie Sutton for technical assistance, Margarete Heck, Helen Strutt, Carl Smythe, Ian Adams, Nick Hastie, Veronica van Heyningen and other members of the CDBG and HGU for advice and helpful discussions. Elwyn Isaac for hosting K.B. in his lab during this work. S. DasGupta, S. Waddell and Laura Lee for sharing unpublished data. David Glover, Thomas Kaufmann, Christian Lehner, Jordan Raff, Trudy Schupbach, Tin Tin Su, Bill Chia, Bloomington stock center, and Developmental Hybridoma Bank for antibodies and fly stocks; Douglas Stuart and Sandy Bruce for assistance with illustrations. Paul Perry for imaging expertise. This work was supported by an MRC Clinician Scientist Fellowship (A.P.J.) and MRC Centre Development Grant (P.W.I.). K.B. is funded by a White Rose Studentship.

References

- Alderton, G. K., Galbiati, L., Griffith, E., Surinya, K. H., Neitzel, H., Jackson, A. P., Jeggo, P. A. and O'Driscoll, M. (2006). Regulation of mitotic entry by microcephalin and its overlap with ATR signalling. *Nat. Cell Biol.* **8**, 725–733.
- Altschul, S. F., Gish, W., Miller, W., Myers, E. W. and Lipman, D. J. (1990). Basic local alignment search tool. *J. Mol. Biol.* **215**, 403–410.
- Basto, R., Lau, J., Vinogradova, T., Gardiol, A., Woods, C. G., Khodjakov, A. and Raff, J. W. (2006). Flies without centrioles. *Cell* **125**, 1375–1386.
- Bond, J., Roberts, E., Mochida, G. H., Hampshire, D. J., Scott, S., Askham, J. M., Springell, K., Mahadevan, M., Crow, Y. J., Markham, A. F. et al. (2002). ASPM is a major determinant of cerebral cortical size. *Nat. Genet.* **32**, 316–320.
- Bond, J., Roberts, E., Springell, K., Lizarraga, S., Scott, S., Higgins, J., Hampshire, D. J., Morrison, E. E., Leal, G. F., Silva, E. O. et al. (2005). A centrosomal mechanism involving CDK5RAP2 and CENPJ controls brain size. *Nat. Genet.* **37**, 353–355.
- Cox, J., Jackson, A. P., Bond, J. and Woods, C. G. (2006). What primary microcephaly can tell us about brain growth. *Trends Mol. Med.* **12**, 358–366.
- Davis, I. (2000). Imaging fluorescence in thick *Drosophila* specimens. In *Protein Localization using Fluorescence Microscopy: A Practical Approach* (ed. V. Allan), pp. 133–162. Oxford: Oxford University Press.

- do Carmo Avides, M. and Glover, D. M. (1999). Abnormal spindle protein, Asp, and the integrity of mitotic centrosomal microtubule organizing centers. *Science* **283**, 1733-1735.
- Edgar, B. A., Sprenger, F., Duronio, R. J., Leopold, P. and O'Farrell, P. H. (1994). Distinct molecular mechanism regulate cell cycle timing at successive stages of *Drosophila* embryogenesis. *Genes Dev.* **8**, 440-452.
- Evans, P. D., Anderson, J. R., Vallender, E. J., Choi, S. S. and Lahn, B. T. (2004). Reconstructing the evolutionary history of microcephalin, a gene controlling human brain size. *Hum. Mol. Genet.* **13**, 1139-1145.
- Freeman, M., Nusslein-Volhard, C. and Glover, D. M. (1986). The dissociation of nuclear and centrosomal division in gnu, a mutation causing giant nuclei in *Drosophila*. *Cell* **46**, 457-468.
- Gabler, M., Volkmar, M., Weinlich, S., Herbst, A., Dobberthien, P., Sklarss, S., Fanti, L., Pimpinelli, S., Kress, H., Reuter, G. et al. (2005). Trans-splicing of the mod(mdg4) complex locus is conserved between the distantly related species *Drosophila melanogaster* and *D. virilis*. *Genetics* **169**, 723-736.
- Gonzalez, C., Saunders, R. D., Casal, J., Molina, I., Carmena, M., Ripoll, P. and Glover, D. M. (1990). Mutations at the *asp* locus of *Drosophila* lead to multiple free centrosomes in syncytial embryos, but restrict centrosome duplication in larval neuroblasts. *J. Cell Sci.* **96**, 605-616.
- Hsu, L. C. and White, R. L. (1998). BRCA1 is associated with the centrosome during mitosis. *Proc. Natl. Acad. Sci. USA* **95**, 12983-12988.
- Huang, J. and Raff, J. W. (1999). The disappearance of cyclin B at the end of mitosis is regulated spatially in *Drosophila* cells. *EMBO J.* **18**, 2184-2195.
- Huyton, T., Bates, P. A., Zhang, X., Sternberg, M. J. and Freemont, P. S. (2000). The BRCA1 C-terminal domain: structure and function. *Mutat. Res.* **460**, 319-332.
- Jackson, A. P., Eastwood, H., Bell, S. M., Adu, J., Toomes, C., Carr, I. M., Roberts, E., Hampshire, D. J., Crow, Y. J., Mighell, A. J. et al. (2002). Identification of microcephalin, a protein implicated in determining the size of the human brain. *Am. J. Hum. Genet.* **71**, 136-142.
- Jeffers, L. J., Coull, B. J., Stack, S. J. and Morisson, C. G. (2007). Distinct BRCT domains in Mcph1/Bril1 mediate ionizing radiation-induced focus formation and centrosomal localization. *Oncogene* doi:10.1038/sj.onc.1210595.
- Kramer, A., Mailand, N., Lukas, C., Syljuasen, R. G., Wilkinson, C. J., Nigg, E. A., Bartek, J. and Lukas, J. (2004). Centrosome-associated Chk1 prevents premature activation of cyclin-B-Cdk1 kinase. *Nat. Cell Biol.* **6**, 884-891.
- Lehmann, R. and Tautz, D. (1994). In situ hybridization to RNA. *Methods Cell Biol.* **44**, 575-598.
- Lin, S. Y., Rai, R., Li, K., Xu, Z. X. and Elledge, S. J. (2005). BRIT1/MCPH1 is a DNA damage responsive protein that regulates the Brca1-Chk1 pathway, implicating checkpoint dysfunction in microcephaly. *Proc. Natl. Acad. Sci. USA* **102**, 15105-15109.
- Maines, J. Z. and Wasserman, S. A. (1999). Post-transcriptional regulation of the meiotic Cdc25 protein Twine by the Dazl orthologue Boule. *Nat. Cell Biol.* **3**, 171-174.
- Manke, I. A., Lowery, D. M., Nguyen, A. and Yaffe, M. B. (2003). BRCT repeats as phosphopeptide-binding modules involved in protein targeting. *Science* **302**, 636-639.
- Martinez-Campos, M., Basto, R., Baker, J., Kernan, M. and Raff, J. W. (2004). The *Drosophila* pericentrin-like protein is essential for cilia/flagella function, but appears to be dispensable for mitosis. *J. Cell Biol.* **165**, 673-683.
- McCreary, B. D., Rossiter, J. P. and Robertson, D. M. (1996). Recessive (true) microcephaly: a case report with neuropathological observations. *J. Intellect. Disabil. Res.* **40**, 66-70.
- Megraw, T. L., Li, K., Kao, L. R. and Kaufman, T. C. (1999). The centrosomin protein is required for centrosome assembly and function during cleavage in *Drosophila*. *Development* **126**, 2829-2839.
- Megraw, T. L., Kao, L. R. and Kaufman, T. C. (2001). Zygotic development without functional mitotic centrosomes. *Curr. Biol.* **11**, 116-120.
- Nakai, K. and Horton, P. (1999). PSORT: a program for detecting sorting signals in proteins and predicting their subcellular localization. *Trends Biochem. Sci.* **24**, 34-36.
- Neitzel, H., Neumann, L. M., Schindler, D., Wirges, A., Tonnie, H., Trimborn, M., Krebsova, A., Richter, R. and Sperling, K. (2002). Premature chromosome condensation in humans associated with microcephaly and mental retardation: a novel autosomal recessive condition. *Am. J. Hum. Genet.* **70**, 1015-1022.
- Northcutt, R. G. and Kaas, J. H. (1995). The emergence and evolution of the mammalian neocortex. *Trends Neurosci.* **18**, 373-379.
- Raff, J. W. and Glover, D. M. (1988). Nuclear and cytoplasmic mitotic cycles continue in *Drosophila* embryos in which DNA synthesis is inhibited with aphidicolin. *J. Cell Biol.* **107**, 2009-2019.
- Raff, J. W., Jeffers, K. and Huang, J. Y. (2002). The roles of Fzy/Cdc20 and Fzr/Cdh1 in regulating the destruction of cyclin B in space and time. *J. Cell Biol.* **157**, 1139-1149.
- Rai, R., Dai, H., Multani, A. S., Li, K., Chin, K., Gray, J., Lahad, J. P., Liang, J., Mills, G. B., Meric-Bernstam, F. et al. (2006). BRIT1 regulates early DNA damage response, chromosomal integrity, and cancer. *Cancer Cell* **10**, 145-157.
- Riparbelli, M. G., Callaini, G., Glover, D. M. and Avides Mdo, C. (2002). A requirement for the Abnormal Spindle protein to organise microtubules of the central spindle for cytokinesis in *Drosophila*. *J. Cell Sci.* **115**, 913-922.
- Sibon, O. C., Laurencon, A., Hawley, R. and Theurkauf, W. E. (1999). The *Drosophila* ATM homologue Mei-41 has an essential checkpoint function at the midblastula transition. *Curr. Biol.* **9**, 302-312.
- Su, T. T. (2000). Immunoblotting of proteins from single *Drosophila* embryos. In *Drosophila Protocols* (ed. W. Sullivan, M. Ashburner and R. S. Hawley), pp. 577-583. New York: Cold Spring Harbor Laboratory Press.
- Su, T. T., Campbell, S. D. and O'Farrell, P. H. (1999). *Drosophila* grapes/CHK1 mutants are defective in cyclin proteolysis and coordination of mitotic events. *Curr. Biol.* **9**, 919-922.
- Sullivan, W., Ashburner, M. and Hawley, R. S. (2000). *Drosophila Protocols*. New York: Cold Spring Harbor Laboratory Press.
- Swan, A., Barcelo, G. and Schupbach, T. (2005). *Drosophila* Cks30A interacts with Cdk1 to target Cyclin A for destruction in the female germline. *Development* **132**, 3669-3678.
- Trimborn, M., Bell, S. M., Felix, C., Rashid, Y., Jafri, H., Griffiths, P. D., Neumann, L. M., Krebs, A., Reis, A., Sperling, K. et al. (2004). Mutations in microcephalin cause aberrant regulation of chromosome condensation. *Am. J. Hum. Genet.* **75**, 261-266.
- Trimborn, M., Schindler, D., Neitzel, H. and Hirano, T. (2006). Misregulated chromosome condensation in MCPH1 primary microcephaly is mediated by condensin II. *Cell Cycle* **5**, 322-326.
- Vaizel-Ohayon, D. and Schejter, E. D. (1999). Mutations in centrosomin reveal requirements for centrosomal function during early *Drosophila* embryogenesis. *Curr. Biol.* **9**, 889-898.
- Wakefield, J. G., Huang, J. Y. and Raff, J. W. (2000). Centrosomes have a role in regulating the destruction of cyclin B in early *Drosophila* embryos. *Curr. Biol.* **10**, 1367-1370.
- Wang, Y.-q. and Su, B. (2004). Molecular evolution of microcephalin, a gene determining human brain size. *Hum. Mol. Genet.* **13**, 1131-1137.
- Wood, B. and Collard, M. (1999). The human genus. *Science* **284**, 65-71.
- Woods, C. G., Bond, J. and Enard, W. (2005). Autosomal recessive primary microcephaly (MCPH): a review of clinical, molecular, and evolutionary findings. *Am. J. Hum. Genet.* **76**, 717-728.
- Xu, X., Lee, J. and Stern, D. F. (2004). Microcephalin is a DNA damage response protein involved in regulation of CHK1 and BRCA1. *J. Biol. Chem.* **279**, 34091-34094.
- Yu, X., Chini, C. C., He, M., Mer, G. and Chen, J. (2003). The BRCT domain is a phospho-protein binding domain. *Science* **302**, 639-642.
- Zhong, X., Pfeifer, G. P. and Xu, X. (2006). Microcephalin encodes a centrosomal protein. *Cell Cycle* **5**, 457-458.